Development of a Traction Control System Using a Special Type of Sliding Mode Controller for Hybrid 4WD Vehicles

Kyoungseok Han, Mooryong Choi, Byunghwan Lee, and Seibum B. Choi, *Member, IEEE*

***Abstract*—Using a special type of sliding mode controller, a new type of traction control system (TCS) for hybrid four-wheel drive vehicles is developed. This paper makes two major contributions. First, a new electric powertrain architecture with an in-wheel motor at the front wheels and a clutch on the rear of the transmission is proposed for maximum traction force. The in-wheel motors are controlled to cycle near the optimal slip point. Based on the cycling patterns of the front wheels, the desired wheel speed for rear wheel is defined. The rear wheels are controlled to track this defined speed by controlling the clutch torque. Unlike conventional TCS algorithms, the proposed method exploits clutch control instead of brake control. Second, a special type of sliding mode controller which uses a nonlinear characteristic of the tire is proposed. An important distinction between the proposed sliding mode control method and other conventional feedback controllers is that the former does not depend on feedback error but provides the same functionality. Therefore, the practical aspects are emphasized in this paper. The developed method is confirmed in simulations, and the results reveal that the proposed method opens up opportunities for new types of TCS.**

***Index Terms*—Hybrid 4WD, in-wheel motor, sliding mode control, traction control system.**

I. Introduction

OVER the past few decades, fuel economy improvements have been a major concern in the field of electric propulsion systems [1]–[3]. However, as the demand for high-performance vehicles has increased over time, automakers have introduced a new type of powertrain architecture for electric and hybrid vehicles. Among such systems, the electric-four wheel drive (E-4WD) system drives two wheels with an electric motor to supplement the traction force, with the other two wheels driven by a conventional internal combustion engine [4].

The goal of this paper is to develop a novel traction control system (TCS) with this electric powertrain architecture. In particular, in-wheel motors (IWMs) are used to create the 4WD system. Compared with conventional vehicles, this electric powertrain configuration introduces new opportunities for new vehicle chassis control systems for the reasons outlined below [5], [6].

It is well known that the dynamic response of a motor arises much more rapidly than that of a conventional internal combustion engine with a hydraulic friction brake for chassis control. In addition, the motor as a chassis control actuator has significantly lower operating delay, which enables accurate wheel slip control. Regarding an in-wheel motor, there is no adverse effect on the driveshaft stiffness given that the motor is directly attached to the wheel.

In addition to the advantages mentioned above, this paper exploits a clutch control technique to limit the torque transmitted from the engine. In order to prevent excessive wheel slippage, conventional TCS algorithms [7]–[9] apply braking force to compensate for excessively transmitted engine torque. At the same time, engine torque reduction control is conducted. However, an inappropriate amount of braking force can cause instability of the vehicle, making it very difficult to realize both a reduction of the engine torque and the generation of braking force simultaneously.

For this reason, a clutch between the engine and the wheels is utilized in this paper instead of braking force control. In most previous studies [10], [11], the clutch of a hybrid vehicle was considered only for mode changes. However, accurate control of the torque transmitted to the drive wheels is possible if clutch control is conducted appropriately.

The ultimate goal of TCS is to provide the vehicle with maximum acceleration by adjusting individual wheel slips. This condition can be achieved when all wheels remain at the optimal wheel slip point. However, it is challenging to control individual wheel slips optimally because sufficient information about the road surface is typically not available. That is, the most challenging issue in relation to TCS algorithms is to identify the road

Manuscript received March 13, 2017; revised July 2, 2017 and August 14, 2017; accepted September 7, 2017. Date of publication September 15, 2017; date of current version January 15, 2018. This work was supported in part by Hyundai Motor Company; in part by the National Research Foundation of Korea funded by the Korean Government (MSIP) under Grant 2017R1A2B4004116; in part by the Technological Innovation R&D Program of SMBA (S2341501); in part by the Ministry of Science, ICT, and Future Planning, South Korea, under the Information Technology Research Center support program supervised by the Institute for Information and Communications Technology Promotion under Grant IITP-2017-2012-0-00628; and in part by the BK21+ Program through the NRF funded by the Ministry of Education of Korea. The review of this paper was coordinated by the Guest Editors of the VPPC 2016 Special Section. *(Corresponding author: Seibum B. Choi.)*

K. Han and S. B. Choi are with the Korea Advanced Institute of Science and Technology, Daejeon 305-806, South Korea (e-mail: hks8804@kaist.ac.kr; sbchoi@kaist.ac.kr).

M. Choi and B. Lee are with Hyundai Motors Group, Seoul 151-742, South Korea (e-mail: mucho@hyundai.com; bhlee1060@hyundai.com).

Color versions of one or more of the figures in this paper are available online at http://ieeexplore.ieee.org.

Digital Object Identifier 10.1109/TVT.2017.2752704

0018-9545 © 2017 IEEE. Personal use is permitted, but republication/redistribution requires IEEE permission.
See http://www.ieee.org/publications_standards/publications/rights/index.html for more information.

Authorized licensed use limited to: Korea Advanced Inst of Science & Tech - KAIST. Downloaded on March 06,2020 at 11:08:26 UTC from IEEE Xplore. Restrictions apply.

surface condition in real time. Although numerous efforts have been made to resolve this issue [12]–[15], none have presented satisfactory results.

In this paper, a special type of sliding mode control method is introduced. Unlike previous methods, the proposed controller does not require real-time road surface information. This approach, a core contribution of this paper, is possible due to the proposed special type of sliding mode control method.

Unlike most other control methods, the sliding controller requires only the sign value of the tracking error, which usually causes control chattering. Although many previous studies have attempted to avoid this chattering [16], but this paper exploits the chattering to define the optimal wheel slip. This is why the sliding control method is adopted in this paper.

The IWMs are controlled such that they are cycled near the optimal slip point by continuous feedback. By monitoring the real-time tire force and wheel speed rate, the desired wheel slip point is determined. Using the optimal wheel slip point determined from the IWM cycling control technique, the rear wheels are also controlled to track the desired slip point. The torque applied to the rear wheels is determined by the clutch and through engine control.

This novel method is possible due to the proposed electric powertrain architecture and the rapid response of the IWM compared to that of a conventional drivetrain.

The rest of this paper proceeds as follows. The proposed powertrain architecture is discussed in Section II. The practical issues pertaining to a conventional TCS algorithm are reviewed in Section III. The core contribution of this paper, i.e., controlling the IWMs, clutch, and engine, is described in Sections IV and V. Section VI presents an overview of the algorithm, and the proposed algorithm is verified in Section VII. Finally, the paper is concluded in Section VIII.

II. Hybrid 4WD Powertrain Architecture

The powertrain architecture discussed here is described in Fig. 1. It is very similar to the conventional parallel hybrid system, but with two primary differences. First, the IWMs are attached to the front wheels to create a 4WD system. The rear wheels are driven by a combination of engine torque and motor/generator (M/G) torque. In general, the E-4WD system is created by a central motor attached to the driveshaft. Therefore, the adverse effect of the driveshaft stiffness should be considered when delivering the motor torque. However, the IWMs are free from these adverse effects given that the motor torque is directly transmitted to the wheels. Second, the clutch is repositioned between the transmission and the rear wheels for the novel TCS algorithm. The operating mode of the conventional parallel hybrid vehicle changes through clutch engagement/disengagement control between the engine and the M/G. For example, if the clutch is completely disengaged, the vehicle can be driven only by the M/G in what is known as the electric vehicle (EV) mode. In this case, however, the torque loss due to the driveshaft must be taken into account; therefore, the amount of transmitted wheel torque cannot be calculated accurately. Moreover, control actuation delay is inevitable in

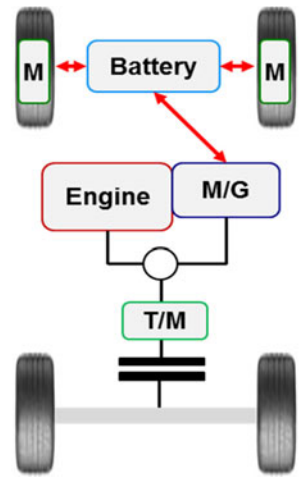

Fig. 1. Hybrid four wheel drive system using IWMs. Fig. 1. Magnetization as a function of applied field. Note that "Fig." is abbreviated. There is a period after the figure number, followed by two spaces. It is good practice to explain the significance of the figure in the caption.

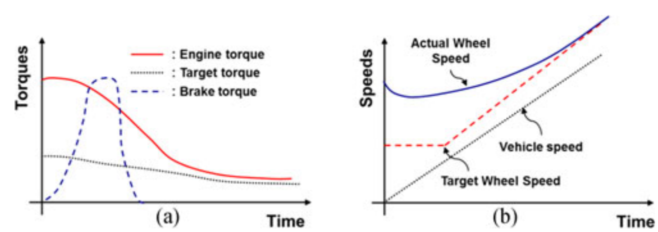

Fig. 2. Typical data trace of a conventional TCS.

the conventional parallel hybrid system. For these reasons, most previous studies did not consider a hybrid or electric powertrain during the development of a chassis control system.

In this paper, however, the proposed electric powertrain configuration is used to develop a chassis control system while maintaining the functionality of the existing hybrid vehicle. For example, various operating modes can be realized using the introduced IWMs and clutch. If the IWMs operate alone and the clutch is disengaged, the vehicle can be switched to the EV mode. Additionally, a rear-wheel-drive system is realized when the IWMs are off and the clutch is engaged.

This paper presents a new TCS algorithm using the rapid response of the IWMs and the clutch.

Moreover, in order to consider certain practical aspects, the pure time delay, actuator bandwidth, and time constant are considered.

III. Conventional TCS

In this section, the practical issues pertaining to a conventional TCS control algorithm are reviewed and the direction of improvement of the TCS is presented.

In a conventional TCS algorithm, the control inputs applied to the drive wheels consist of the engine torque and the brake torque. Fig. 2 depicts the typical torque data trace of a conventional TCS. Because the TCS generally operates under full-throttle acceleration, the engine torque initially increases

Authorized licensed use limited to: Korea Advanced Inst of Science & Tech - KAIST. Downloaded on March 06,2020 at 11:08:26 UTC from IEEE Xplore. Restrictions apply.

rapidly. However, the excessive torque transmitted to the drive wheel due to full-throttle acceleration does not allow maximum tire adhesion between the tire and the surface of the road. That is, an appropriate amount of engine torque should be transmitted to the drive wheels while controlling the engine throttle angle. However, the engine torque cannot be reduced immediately because the engine dynamic response very slowly copes with the rapid wheel dynamics, as shown in Fig. 2(a). As the figure shows, the engine torque is reduced very slowly. Thus, brake control, which provides a rapid dynamic response, is used to reduce the transmitted torque to the drive wheels. At the same time, the engine torque decreases until it reaches the target torque.

This is a typical method used by conventional TCS algorithms. Typical trajectories of the wheel speeds obtained as a result of engine and brake control are exhibited in Fig. 2(b).

However, it is very difficult to control both the engine torque and the brake torque simultaneously. Because the reduction of the engine torque and the generation of braking torque should occur at the same time, highly accurate control algorithm tuning is required to track the desired target wheel speed. Even when the algorithm is perfectly tuned, there are some inherent deficiencies. As mentioned in Section I, there are no sufficient sensor signals in production vehicles, making it difficult to identify road surface conditions accurately. That is, the target wheel speed in Fig. 2(b) is not actually given when activating the TCS. In addition, because there is no vehicle speed sensor in production vehicles, the current vehicle speed in Fig. 2(b) is also not provided.

In summary, unlike the conventional feedback control algorithm, the current state as well as the desired state are not given. This is the main reason why feedback control is not easily realized when developing a TCS algorithm.

For these reasons, many automakers exploit rule-based control algorithms that consider as much data as possible to manage numerous practical concerns. However, rule-based algorithms generally cause a computational burden and limit the control performance for safety issues.

In order to solve these problems, a new powertrain configuration and control algorithm is presented in this paper, as described in the following sections.

IV. In-Wheel Motor Cycling Control

A. Nonlinear Tire Force Curve

Tire slip during acceleration is defined as follows [17],

$$\lambda = \frac{Rw - V_{car}}{Rw}, \tag{1}$$

where *R* is the wheel effective radius, *w* is the wheel angular velocity, and V_{car} is the absolute vehicle velocity.

It is well known that the relationship between the tire force and tire slip is nonlinear, as depicted in Fig. 3. The tire force curve remains linear until the slip reaches the optimal slip, λ_{opt}. However, the instantaneous slope exhibits nonlinearity near the optimal slip, and it is exactly zero at the point of optimal slippage.

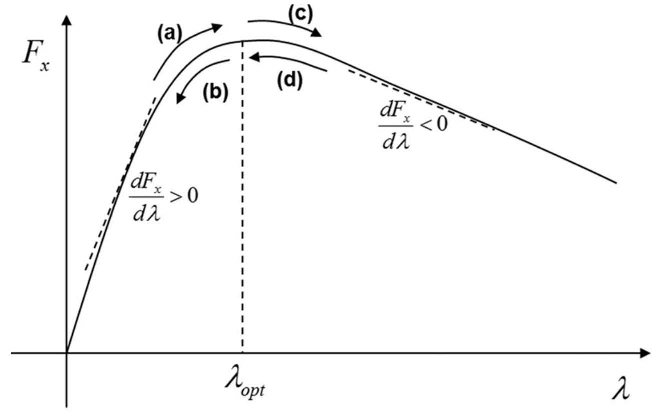

Fig. 3. Nonlinear tire force curve.

It must be noted again that the ultimate goal of the TCS is to keep the individual wheel slips at the optimal slip point when the vehicle accelerates in a straight line. However, because the optimal slip point depends on the condition of the road surface, it is not actually given. In addition, because the absolute vehicle velocity cannot be measured, it is difficult to identify the current slip in real time.

The instantaneous slope of the tire force curve can be written as follows [18],

$$\frac{dF_x}{d\lambda} = \frac{dF_x/dt}{d\lambda/dt} = \frac{\dot{F}_x}{\dot{\lambda}}, \tag{2}$$

where F_x is the longitudinal tire force.

Therefore, the instantaneous slope of the tire force curve can be expressed as the ratio between the time derivative of the tire force and the time derivative of the slip.

The time derivative of the tire slip is expressed as (3) assuming that the vehicle velocity is a slowly varying parameter.

$$\dot{\lambda} = \frac{d\lambda}{dt} = \frac{d}{dt}\left(\frac{Rw - V_{car}}{Rw}\right) = \frac{V_{car}\dot{w}}{Rw^2}, \tag{3}$$

Using (3), the instantaneous slope of tire force curve is given as follows:

$$\frac{dF_x}{d\lambda} = \frac{\dot{F}_x}{\dot{\lambda}} = \frac{Rw^2\dot{F}_x}{V_{car}\dot{w}}. \tag{4}$$

If $\dot{w}$ and $\dot{F}_x$ can be accurately measured or at least estimated, the TCS strategy is easily constructed. That is, the drive wheels are controlled such that (4) approaches zero. However, the time derivative of the sensor signals is influenced significantly by the measurement noise effect. Therefore, the direct use of (4) cannot provide reliable results. For this reason, this paper indirectly uses (4).

Note that the signs of $\dot{\lambda}$ and $\dot{w}$ are identical, as indicated by (3). In addition, the signs of the product of the time derivative of the tire force and the wheel speed are divided based on the optimal slip, as depicted in Table I. That is, sgn $\dot{F}_x\ \dot{w}$ is positive before the slip reaches the optimal slip but is negative in the opposite region, as described in Fig. 3.

Based on this, a special type of sliding mode control method is presented in the following sections.

Authorized licensed use limited to: Korea Advanced Inst of Science & Tech - KAIST. Downloaded on March 06,2020 at 11:08:26 UTC from IEEE Xplore. Restrictions apply.

TABLE I
THE SIGNS OF THE TIME DERIVATIVE OF TIRE FORCE AND WHEEL SPEED

Areas	sgn $(\dot{F}_x)$	sgn $(\dot{w})$	sgn $(\dot{F}_x \dot{w})$
(a)	+	+	+
(b)	−	−	+
(c)	−	+	−
(d)	+	−	−

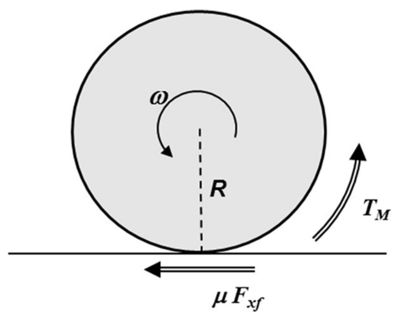

Fig. 4. Diagram of front wheel.

B. Tire Force Observer

In order to determine $\dot{w}$ and $\dot{F}_x$ at the same time, a tire force observer is proposed in this section.

A diagram of a front wheel control system is depicted in Fig. 4, and the wheel dynamics can be expressed as follows,

$$J_f \dot{w}_f = T_M - RF_{xf}, \tag{5}$$

where J_f is the front wheel rotational inertia, w_f is the front wheel angular velocity, T_M is the motor torque, and F_{xf} is the front longitudinal tire force.

Using an unknown input observer (UIO), the tire force can be estimated as follows [12],

$$\dot{\hat{w}}_f = \frac{1}{J_f} T_M - \frac{R}{J_f} \hat{F}_{xf} + l_1 (w_f - \hat{w}_f), \tag{6}$$

$$\dot{\hat{F}}_{xf} = -l_2 (w_f - \hat{w}_f), \tag{7}$$

where l_1 and l_2 are the positive observer gains.

For choosing the observer gain, the following must be satisfied:

$$l_1 > C_{e1} \geq \|v\|_1. \tag{8}$$

where

$$v(t) = \frac{R\tilde{F}_{xf}}{J_f \tilde{w}_f}. \tag{9}$$

whose greatest $L1$-norm over all t is upper bounded by a positive constant C_{e1}. This is reasonable because the magnitudes of the estimation error are physically limited [19]. Also, the amount of selected gain is used to demonstrate the overall stability of the proposed controller in the next sub-section.

As indicated in (6) and (7), $\dot{\hat{w}}_f$ and $\dot{\hat{F}}_{xf}$ can be estimated at the same time. In this paper, these estimates are used instead of the measured wheel speed and tire force. Because the proposed algorithm is simply based on the signs of $\dot{w}$ and $\dot{F}_x$, very accurate signs of $\dot{w}_f$ and $\dot{F}_{xf}$ are required. However, these signs are significantly influenced by the randomly imposed measurement noise. Therefore, the direct use of measured values is excluded in this study.

However, given that the proposed observers in (6) and (7) are strongly related to each other, the sign of the product of these values can have a consistent value according to the applied motor torques. This explains why this approach is adopted here, and this is the basis of the proposed special type of sliding mode controller.

The stability of the designed observers can be analyzed using the error dynamics.

The error dynamics for the wheel dynamic is as follows,

$$J_f \dot{\tilde{w}}_f = -R\tilde{F}_{xf} - l_1 \tilde{w}_f, \tag{10}$$

where $\tilde{w}_f = w_f - \hat{w}_f$.

Differentiating (10) with respect to time results in

$$J_f \ddot{\tilde{w}}_f = -R\dot{\tilde{F}} - l_1 \dot{\tilde{w}}_f. \tag{11}$$

Assuming that the longitudinal tire force is a slowly varying parameter and substituting (7) into (11) leads to

$$J_f \ddot{\tilde{w}}_f + l_1 \dot{\tilde{w}}_f + R l_2 \tilde{w}_f = 0. \tag{12}$$

Therefore, $\tilde{w}_f$ converges to zero by adjusting the observer gains.

C. Special Type of Sliding Mode Controller

In this section, a special type of sliding mode control method using IWMs, the core contribution of the paper, is proposed. In order to achieve the goal of the TCS, a switching surface is defined as [16]

$$S(t) = \lambda_f - \lambda_{opt}. \tag{13}$$

Using this switching surface, the following desired motor torque is constructed:

$$\begin{aligned} u = T_M &= R\hat{F}_{xf} + J_f \frac{Rw_f^2}{V_{car}} \dot{\lambda}_{f,opt} \\ &\quad - K \frac{J_f R w_f^2}{V_{car}} \cdot \mathrm{sgn}(\lambda_f - \lambda_{opt}), \end{aligned} \tag{14}$$

where K is the positive control gain, and $\hat{F}_{xf}$ is the estimated tire force at the front wheels in (7).

The control gain must satisfy the following condition:

$$K > C_{e2} \geq \left\| v \cdot \frac{\tilde{w}_f V_{car}}{R w_f^2} \right\|_1. \tag{15}$$

Similar to the observer gain, the control gain is also upper bounded by a positive constant C_{e2} with knowing that the magnitudes of each element in (15).

In order to demonstrate the stability of the proposed controller in (14), the Lyapunov function candidate is determined as follows:

$$V = \frac{1}{2} S^2 + \frac{1}{2} \tilde{w}_f^2 \tag{16}$$

Authorized licensed use limited to: Korea Advanced Inst of Science & Tech - KAIST. Downloaded on March 06,2020 at 11:08:26 UTC from IEEE Xplore. Restrictions apply.

In order to ensure the asymptotic stability of (12), the following condition must be satisfied:

$$\dot{V} < 0 \,\text{for}\, S \neq 0 \tag{17}$$

The derivative of V is calculated as follows:

$$\dot{V} = S\left(\dot{\lambda}_f - \dot{\lambda}_{f,opt}\right) + \tilde{w}_f\left(\dot{w}_f - \dot{\hat{w}}_f\right) \tag{18}$$

Substituting (3), (5), (6) and (14) into (18) leads to

$$\begin{aligned}\dot{V} &= \left[\frac{V_{car}}{Rw_f^2}\left(\frac{T_M}{J_f} - \frac{RF_{xf}}{J_f}\right) - \dot{\lambda}_{f,opt}\right] + \tilde{w}_f\left(\dot{w}_f - \dot{\hat{w}}_f\right) \\ &= -K\cdot S\mathrm{sgn}(S) - l_1\tilde{w}_f^2 + \frac{\tilde{F}_{xf}}{J_f\tilde{w}_f}\left(\frac{\tilde{w}_f V_{car}}{w_f^2}S - R\tilde{w}_f^2\right). \\ &\leq 0 \quad \because (8)\text{ and }(15)\end{aligned} \tag{19}$$

By applying Barbalat's lemma [20], it can be proved that the tracking and estimation errors converge to zero.

This is a conventional sliding mode control technique of the type commonly proposed in the literature. Even if a conventional sliding mode controller is theoretically perfect, it suffers some inherent flaws. As mentioned in the previous sections, λ and λ_{opt} are not provided when the TCS actually operates. Thus, in most previous studies, λ and λ_{opt} are assumed to be known values in real time [21]–[23].

In order to solve these practical issues, this paper proposes a special type of sliding mode controller that does not require the real-time slip or road surface information.

As shown in (14), a sliding mode controller consists of the feed-forward and feedback terms; however, only the sign value of the feedback term is required.

Considering Table I, the following relationship can be obtained:

$$\mathrm{sgn}(\lambda_f - \lambda_{opt}) = -\mathrm{sgn}(\dot{\hat{F}}_{xf}\cdot\dot{w}_f) \tag{20}$$

In addition, $\dot{\lambda}_{opt} = 0$ when the vehicle is traveling on a homogeneous road surface. Moreover, the front longitudinal tire force was estimated in the previous section, and V_{car} is inferred from the wheel speeds with an acceptable degree of error. Also, if the vehicle is on a split road surface where the left and right wheels have the different optimal slip point and maximum force, both IWMs are controlled to track the wheel motion which has a smaller maximum tire force to avoid a yaw moment generation.

At this stage, the conventional sliding mode controller of (14) can be expressed, as follows,

$$u = T_M = R\hat{F}_{xf} + K\frac{J_f Rw_f^2}{\min(Rw_{rl}, Rw_{rr})}\cdot\mathrm{sgn}(\dot{\hat{F}}_{xf}\cdot\dot{w}_f), \tag{21}$$

where w_{rl} and w_{rr} are the rear left and rear right wheel angular velocities.

In (21), there is no tracking error term, but the functionality is identical to that in (14). In addition, (21) does not require slip or road surface information; instead, only the measured wheel speed and estimated tire force are sufficient.

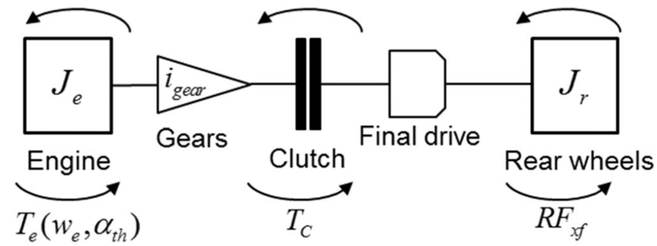

Fig. 5. Representation of the simplified driveline model.

Using (21), the IWMs at the front wheels are cycled independently near the optimal slip point. While cycling the IWMs, the optimal wheel slip amounts are estimated.

In general, control chattering of the sliding mode control method due to the sign function is undesirable in many practical control systems [16]. Therefore, numerous methods have been proposed to avoid control chattering by providing continuous/smooth control signals. However, this paper does not avoid control chattering but rather creates intentional chattering to estimate the optimal slip point.

V. Rear Wheel Slip Control

The cycling pattern of the front wheels is monitored to calculate the desired wheel speed, and the rear wheels are controlled to track this calculated wheel speed. As shown in Fig. 1, the amounts of torque applied to the rear wheels are transmitted from the engine and the clutch. Therefore, the desired torque for the rear wheels can be controlled by the clutch on the rear of the transmission.

The simplified driveline model used for the design of controllers is presented in Fig. 5. Using the torque balance relationships, the driveline model in Fig. 5 can be expressed as follows,

$$J_e\dot{w}_e = T_e(w_e, \alpha_{th}) - T_C, \tag{22}$$

$$J_r\dot{w}_r = T_C - RF_{xr}, \tag{23}$$

where J_e and J_r are the engine and rear wheel rotational inertia, respectively, w_e and w_r are the corresponding engine and rear wheel angular velocities. Additionally, T_e is the engine torque, T_c is the clutch torque, α_{th} is the throttle angle of the engine, and F_{xr} is the rear longitudinal tire force.

The clutch torque while slipping is mathematically represented as follows,

$$T_C = \mu PAR_c, \tag{24}$$

where μ is the clutch surface friction coefficient, P is the hydraulic pressure applied to the clutch plate, A is the effective area of the clutch, and R_c is the effective radius of the clutch.

By controlling both P and T_e simultaneously, the driveline can be controlled to satisfy the goal of the TCS algorithm. Details are described in the following sections.

A. Clutch Torque Control

As described briefly, it is very difficult to control the engine and the brake at the same time in a conventional TCS algorithm.

Authorized licensed use limited to: Korea Advanced Inst of Science & Tech - KAIST. Downloaded on March 06,2020 at 11:08:26 UTC from IEEE Xplore. Restrictions apply.

Therefore, this paper excludes brake control, whereas clutch control is exploited instead. The clutch torque when slipping occurs is calculated from (24), which is valid when the engine crankshaft rotational speed is fast enough. Therefore, a new strategy that controls the clutch and the engine separately can be proposed in this paper. This is possible due to the introduced powertrain architecture, where the clutch is moved to the rear of the transmission.

Since the rapid engagement of the clutch when operating the launch control may deteriorate the durability of clutch and ride quality, a smooth clutch engaging control for approximately 5seconds is widely adopted in automotive manufacturing [24]. In addition, the dynamic response of the clutch is fast enough to regulate the torque transmitted to the drive wheels. Therefore, using a clutch can be a suitable candidate to replace the use of hydraulic brake.

With the desired wheel speed calculated from the cycling control of the IWMs, the adaptive sliding mode control method [25] is used to control the rear wheels.

The sliding surface is defined as a tracking error,

$$s_1 = w_r - w_{rdes}, \tag{25}$$

where w_r is the rear wheel speed and w_{rdes} is the desired rear wheel speed calculated from the cycling control of the IWMs.

The control objective is to choose an appropriate control law such that w_r tracks the w_{rdes}. Therefore, the sliding surface should satisfy the following condition for asymptotic stability,

$$\dot{s}_1 = -\lambda_1 s_1, \tag{26}$$

where λ_1 denotes the positive control gain.

When substituting (23) into (26), the desired clutch torque can then be expressed as follows:

$$T_{Cdes} = R\hat{F}_{xr} + J_r\dot{w}_{rdes} - \lambda_1 J_r(w_r - w_{rdes}) \tag{27}$$

Here, the longitudinal rear tire force is considered to be an unknown parameter. Therefore, the adaptive law is established as follows,

$$\dot{\hat{F}}_{xr} = -k_b\frac{R}{J_r}s_1, \tag{28}$$

where k_b denotes the positive adaptation gain.

Combining (23) and (27),

$$\begin{aligned} J_r\dot{w}_r &= T_{Cdes} - RF_{xr} \\ &= R\tilde{F}_{xr} + J_r\dot{w}_{rdes} - \lambda_1 J_r(w_r - w_{rdes}), \end{aligned} \tag{29}$$

where $\tilde{F}_{xr} = \hat{F}_{xr} - F_{xr}$.

Then,

$$\dot{s}_1 = \frac{R}{J_r}\tilde{F}_{xr} - \lambda_1 s_1, \tag{30}$$

In this way, the desired clutch torque in (27) is used to calculate the target control input *P*.

At this stage we consider a Lyapunov candidate function, as follows:

$$V_1 = \frac{1}{2}s_1^2 + \frac{1}{2k_b}\tilde{F}_{xr}^2 \tag{31}$$

Differentiating the Lyapunov function with respect to time yields

$$\begin{aligned} \dot{V}_1 &= s_1\dot{s}_1 + \frac{1}{k_b}\tilde{F}_{xr}\dot{\hat{F}}_{xr} = s_1\left(\frac{R}{J_r}\tilde{F}_{xr} - \lambda_1 s_1\right) + \frac{1}{k_b}\tilde{F}_{xr}\dot{\hat{F}}_{xr} \\ &= -\lambda_1 s_1^2 + \tilde{F}_{xr}\left(\frac{R}{J_r}s_1 + \frac{1}{k_b}\dot{\hat{F}}_{xr}\right). \end{aligned} \tag{32}$$

If the established adaptive law (28) is substituted into (32), the Lyapunov stability condition in (17) is satisfied.

As described in this section, the engine dynamics is not considered. However, for complete clutch engagement, engine torque reduction control should be conducted independently. In other words, the engine torque should be controlled to track the desired engine speed. This is covered in the next section.

B. Engine Torque Reduction Control

The maximum traction force can be obtained by means of the cycling control of IWMs and control of the clutch torque. However, the engine dynamics should be also considered, as in a conventional TCS algorithm. Because the clutch slip control method adversely affects the durability of a wet clutch, it is not desirable to maintain the slip condition for a long time. Therefore, the clutch on the rear of the transmission should be entirely engaged when the engine torque is sufficiently reduced. From that time, the clutch torque control is omitted in the proposed TCS algorithm, but the engine torque control is conducted only to track the desired wheel speed. Therefore, engine torque reduction control should be performed independently of clutch torque control.

The engine speed should track the desired wheel speed as calculated from cycling control of the IWMs. The desired engine speed is defined as follows considering the gear ratio of the transmission and differential,

$$w_{edes} = i_{gear}w_{rdes}, \tag{33}$$

where w_{edes} represents the desired engine speed and i_{gear} is the lumped gear ratio.

The sliding surface is also defined as a tracking error:

$$s_2 = w_e - w_{edes} \tag{34}$$

Similar to the previous section, the asymptotic stability can be proven if the following condition is met,

$$\dot{s}_2 = -\lambda_2 s_2, \tag{35}$$

where λ_2 is the positive control gain.

Using (22) and (35), the desired engine torque can be calculated as follows:

$$T_{edes} = T_C + J_e\dot{w}_{edes} - \lambda_2 J_e(w_e - w_{edes}) \tag{36}$$

In (36), the clutch torque T_c is provided by (24).

VI. Algorithm Overview

Fig. 6 exhibits the overall structure of the proposed TCS algorithms. The required sensor signals are the wheel speeds, engine speed, and motor torque, which are the measurable signals in

Authorized licensed use limited to: Korea Advanced Inst of Science & Tech - KAIST. Downloaded on March 06,2020 at 11:08:26 UTC from IEEE Xplore. Restrictions apply.

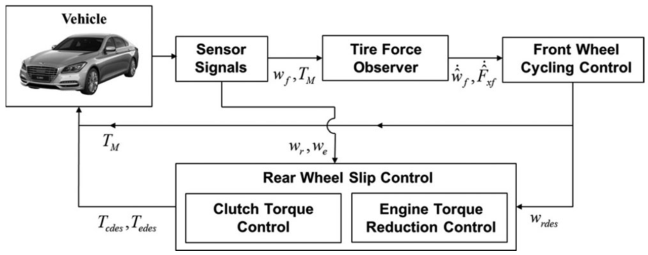

Fig. 6. Overall structure of the proposed TCS algorithm.

TABLE II
VEHICLE SPECIFICATIONS

Parameters	Quantity	Values
J_f, J_r	Rotational inertia of the front and rear wheels	0.6 kg·m^2
R	Wheel effective radius	0.387 m
M_v	Gross vehicle weight	2295 kg
l_f	Distance between the front axle and center of gravity	1.48 m
l_r	Distance between the rear axle and center of gravity	1.533 m
h	Height of center of gravity	0.563 m

production vehicles. Using the estimated results from the tire force observer, the front wheels are independently controlled to cycle near the optimal slip point. At the same time, the clutch on the rear of the transmission and the engine are also controlled to track the desired speed calculated from the cycling control of the front wheels. However, these two controllers operate independently. In summary, the chassis and powertrain systems are controlled by the three control inputs: T_M, T_{edes}, and T_{cdes}. The important point is that these control inputs are independent of each other. Therefore, each controller only has to consider its own dynamics without considering other dynamics. In addition, it is assumed that the motor torque capacity is limited to $[-650\ 650]$ Nm. That is, the IWMs of the front wheels can provide up to 0.3 g of acceleration considering the gross weight of the target vehicle.

VII. Simulation Results

In this section, simulation studies were conducted to verify the effectiveness of the developed algorithm. The vehicle and tire model stored in CarSim, which is a commercial vehicle dynamics solver package, were used. The main CarSim vehicle model parameters are described in Table II. In addition, the used friction model is based on the Magic Formula tire model [26].

Fig. 7 depicts the simulation results on a low-mu road surface when the controllers did not operate. Full-throttle acceleration was applied using the accelerator pedal at $t = 1$ s to generate maximum engine torque. At that time, the clutch is fully engaged. As a result, the product of the engine torque and the gear ratio increased rapidly, as described in Fig. 7(a). However, the engine torque decreased as the engine speed increased due to the characteristics of the engine dynamics. Given that excessive engine torque was transmitted to the rear wheels, the rear wheel speed diverged, as shown in Fig. 7(b), whereas the front wheel speed matched the vehicle speed because they were non-driven wheel. In the simulation environment, the road surface

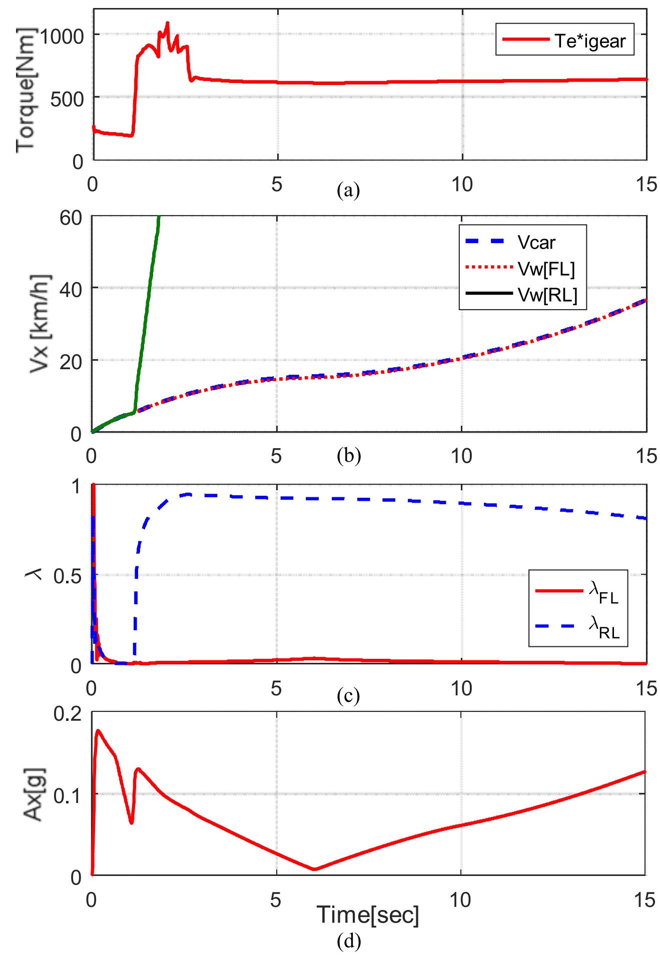

Fig. 7. Plots of simulation results on a low-mu road surface ($\mu = 0.27$) with no control.

friction coefficient was set to 0.27, which represents a low-mu surface. That is, if the wheel slip was very well controlled, the maximum vehicle acceleration could be approximately 0.27 g on this road surface. However, the rear wheels lost its adhesion to the road surface due to the excessive wheel slippage, as exhibited in Fig. 7(c). Moreover, the front wheel slip remained close to zero. Consequently, these wheel slips resulted in insufficient vehicle acceleration, even if the vehicle could accelerate to 0.27 g. Therefore, the developed TCS algorithm can improve the traction performance of a vehicle in these situations.

Similar to the previous simulation case, the vehicle was driven on a low-mu road surface with $\mu = 0.18$ under a full-throttle acceleration condition, as shown in Fig. 8. In this case, however, the wheel slips were controlled using the developed TCS algorithm. The controller activated when the derivative of the front wheel speed exceeded configured threshold. Also, the proposed algorithm was operated with a sampling rate of 0.01 s, but no computational burden was noted. In addition, with commercialization of the proposed algorithm in mind, practical aspects such as the bandwidth, time delay, and slew rate of the actuator were also considered in the simulation environment.

As shown in Fig. 8(a), full-throttle acceleration increased the engine torque rapidly as soon as the vehicle started to

Authorized licensed use limited to: Korea Advanced Inst of Science & Tech - KAIST. Downloaded on March 06,2020 at 11:08:26 UTC from IEEE Xplore. Restrictions apply.

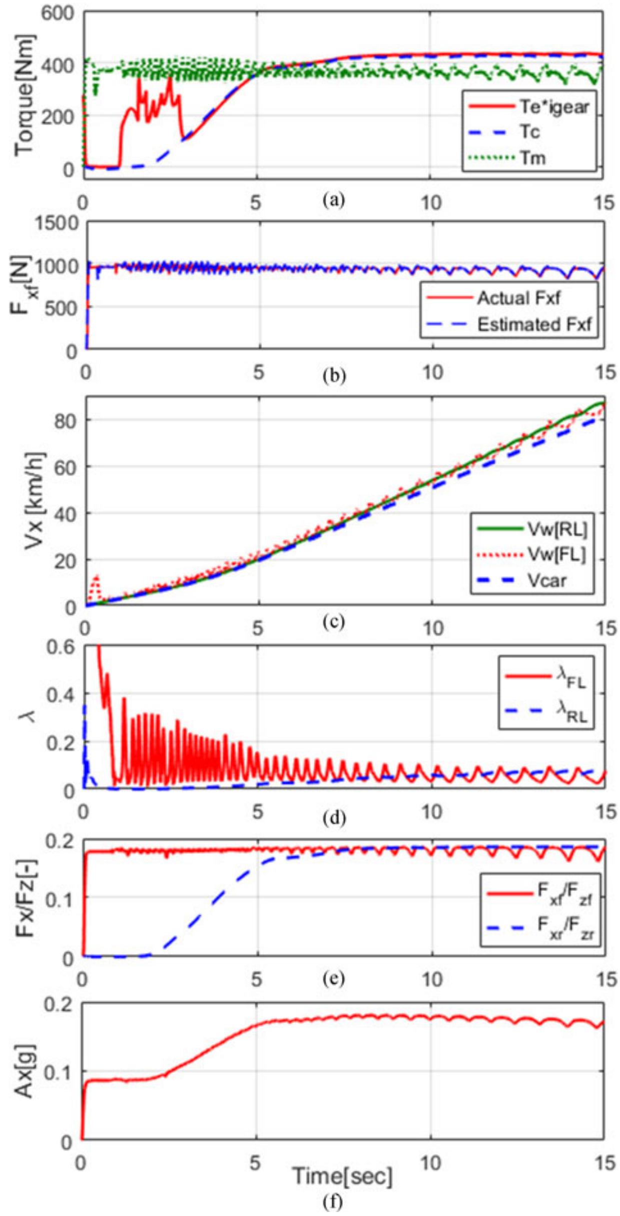

Fig. 8. Plots of simulation results on a low-mu road surface ($\mu = 0.18$).

accelerate, as in the previous case. However, the increased engine torque started to decrease because the engine torque reduction controller attempted to reduce the excessive engine torque. In addition, the torque transmitted to the rear wheels was controlled by the clutch during the engine torque reduction control process, and these two controllers were independent of each other. That is, regardless of the amount of the engine torque, the wet clutch was controlled to transmit an appropriate amount of torque to the rear wheels. Furthermore, the engine torque was controlled independently to track the desired engine speed. As depicted in Fig. 8(a), the product of the engine torque and the gear ratio was nearly identical to the clutch torque from $t = 3$. From then on, engine torque was transmitted directly to the rear wheels, and no clutch slip control was required. Based on (22), the engine speed was decreased when the clutch torque exceeded the product of the engine torque and the gear ratio. These two independent controllers allowed the rear wheels to track the desired wheel speed, as defined from the cycling patterns of the front wheels. Also, it can be observed in Fig. 8(a) that the motor torque is provided for the front wheels to be cycled around the optimal slip point.

It can be argued that changing the direction of the motor frequently can reduce the durability of motor. However, there have been numerous attempts to utilize the motors as actuators when activating the wheel slip controller [5]. Although a precise analysis of the impact of applied torque on motor durability is excluded from the scope of the paper, the use of motors as actuators in TCS operation is feasible when considering these already reported works [5].

Fig. 8(b) exhibits the estimation result of the front tire force, which is an important feedback term in the proposed controller, and indicates that the proposed observer successfully estimates the front tire force.

As depicted in Fig. 8(c), the front wheels were controlled to cycle near the optimal slip point using a special type of sliding mode controller. Considering the physical constraints of the vehicle, the desired wheel speed was defined after smoothing the front wheel speed using a low-pass filter and a rate limiter. As expected, the front wheel slips fluctuated when finding the optimal slip, and the rear wheel slips attempted to track this value, as shown in Fig. 8(d). In addition, Fig. 8(e) shows the normalized forces representing the level of the surface friction used and confirms that each wheel utilized the available friction as much as possible. Owing to the proposed TCS algorithm, the vehicle accelerated up to approximately 0.18 g, which was the maximum acceleration of the vehicle on this road surface, as described in Fig. 8(f).

In addition, the excessive amount of cycling is prevented by introducing a varying control gain which is a function of the vehicle speed. This gain decreases as the vehicle speed increases to reduce the high oscillation. As a result, a ride quality of the vehicle could be improved.

Fig. 9 shows the simulation results when the vehicle was driven quickly onto a different road surface but with the other conditions identical to those in the previous case. The surface transition occurred at $t = 9$ s. The main purpose of this test was to verify the robustness of the algorithm for road surface changes. As shown in Fig. 9(a), the engine and clutch torque were controlled simultaneously to meet the control performance requirements regardless of the surface transition. In addition, it can be confirmed that the motor torque increased at $t = 9$ s to utilize the increased road friction coefficient as much as possible. Because the road surface mu was increased after $t = 9$ s as compared to that in the previous case, the required clutch torque in Fig. 9(a) for rear wheels was larger than that in Fig. 8(a). As shown in the figure, only part of the engine torque was transmitted to the rear wheels by the clutch control, and the engine torque approached the clutch torque over time. As depicted in Fig. 9(b), the estimated tire force tracked the actual force satisfactorily despite the road surface transition.

Fig. 9(c) and (d) illustrate the speed trajectory and wheel slip control performance, respectively, confirming that the basic

Authorized licensed use limited to: Korea Advanced Inst of Science & Tech - KAIST. Downloaded on March 06,2020 at 11:08:26 UTC from IEEE Xplore. Restrictions apply.

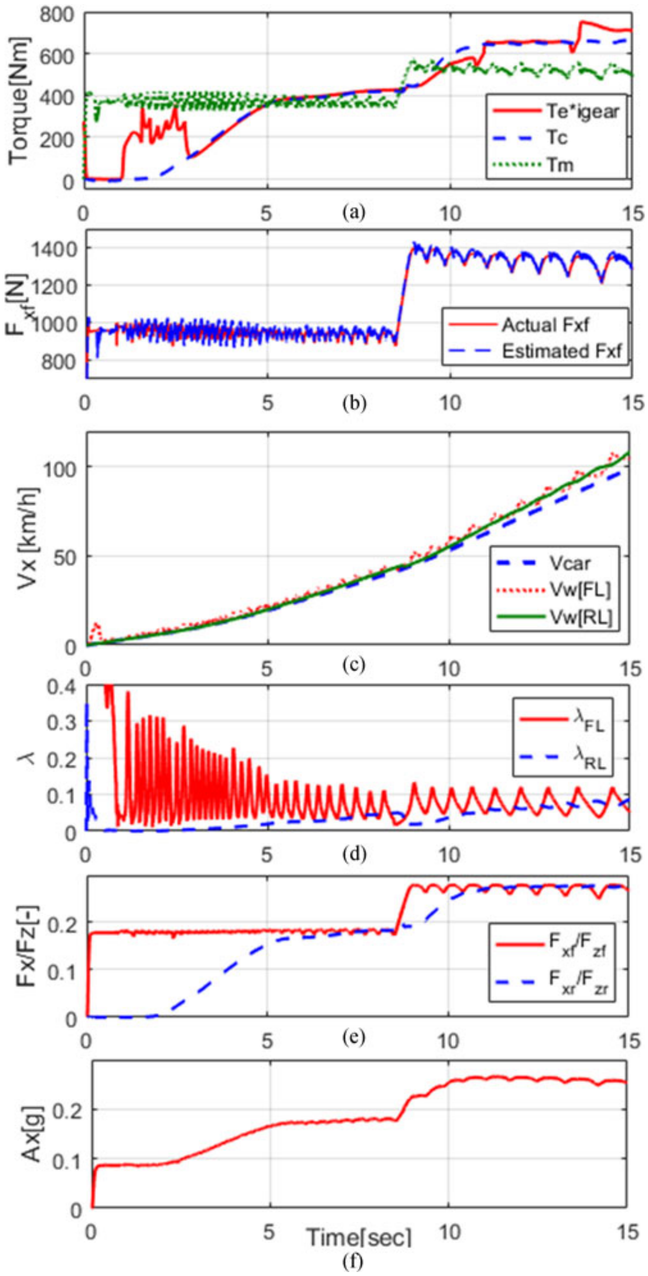

Fig. 9. Plots of simulation results on a road surface transition ($\mu = 0.18 \rightarrow \mu = 0.27$).

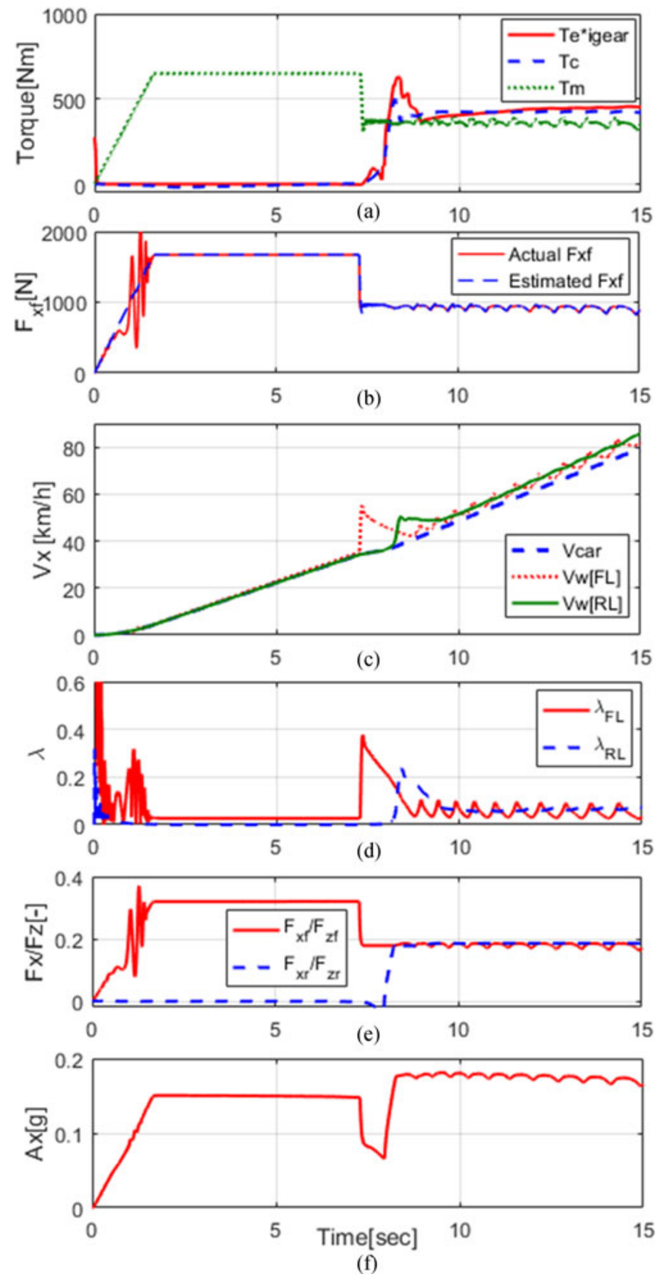

Fig. 10. Plots of simulation results on a road surface transition ($\mu = 0.54 \rightarrow \mu = 0.18$).

principle of the proposed algorithm could be explained well by the results. It can also be concluded from Fig. 9(e) and (f) that the vehicle utilized the road friction coefficient to the greatest extent possible.

The robustness of the developed algorithm was verified in a more severe simulation environment in Fig. 10. As illustrated in Fig. 10(a), the vehicle traveled on a high-mu road surface with only IWMs and entered a low-mu road surface at $t = 7$ s. Since the motor torque capacity was limited to $[-650\ 650]$ Nm, the used surface friction was about 0.3 until surface transition occurred, as depicted in Fig. 10(e). This represents a typical vehicle acceleration on a high-mu surface and there is no need to activate the TCS. However, a large amount of excessive front wheel slip was detected at the surface transition moment, as exhibited in Fig. 10(d). At that time, the developed controllers attempted to find the optimum slip point by reducing the torque input, and the vehicle accelerated while maintaining the slip ratio. Although a sudden reduction of surface friction caused the tires to lose their grips for a while, the proposed method quickly prevented the excessive wheel slip generation.

Fig. 11 describes the simulation results when the vehicle was driven on a low-mu road surface with 2deg road slope. Since the proposed method does not require the road surface information, there is no need to consider additional steps to identify the road slope. Therefore, the robustness of algorithm against the change of road slope could be verified from the results in Fig. 11.

Authorized licensed use limited to: Korea Advanced Inst of Science & Tech - KAIST. Downloaded on March 06,2020 at 11:08:26 UTC from IEEE Xplore. Restrictions apply.

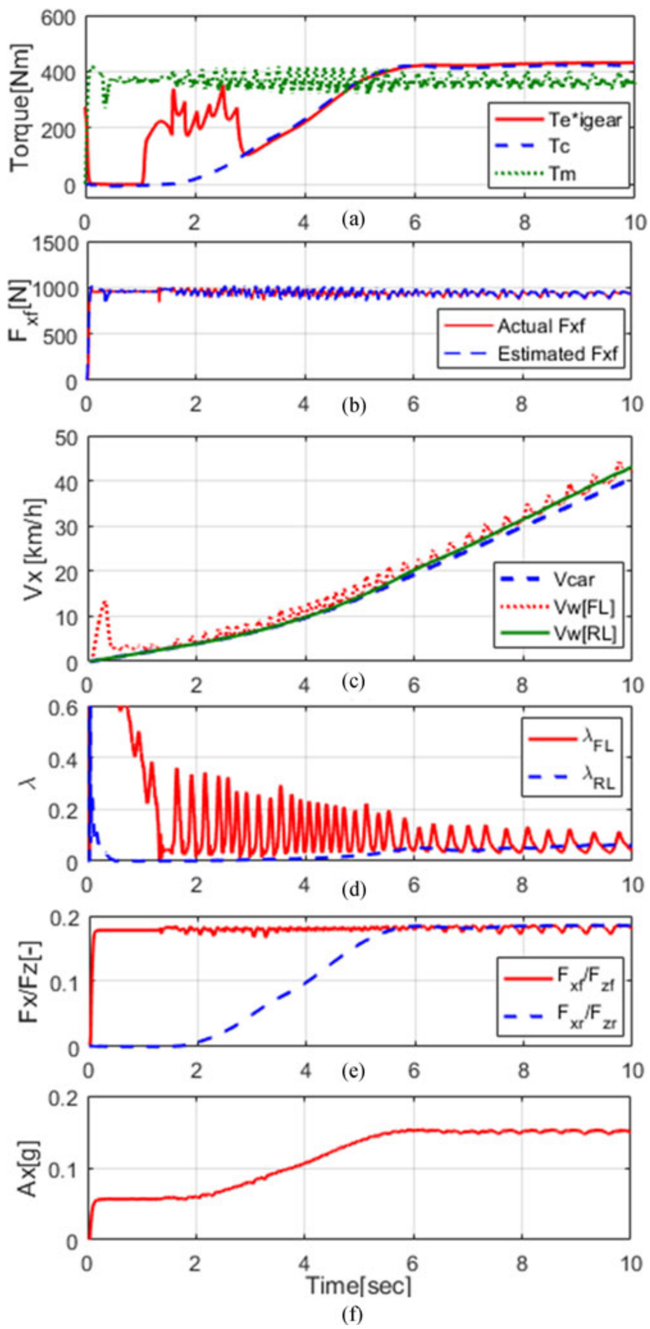

Fig. 11. Plots of simulation results on a low-mu road surface ($\mu = 0.18$) with 2deg road slope.

Although the same actuator torques were applied in Fig. 11(a) and Fig. 8(a), the vehicle in this scenario could not be able to accelerate as much as the acceleration shown in Fig. 8(f) due to the road slope. However, it can be found that the goal of TCS is faithfully performed by monitoring the IWM's cycling patterns and the rear wheel slips in Fig. 11(d). The acceleration performance of the vehicle is depicted in Fig. 11(f).

The performance of the developed controller cannot be directly comparable to the performance of previous studies in [21]–[23] because the surface conditions, tires, vehicle type, and experimental conditions are all different. However, it can be said that the vehicle makes the most of the surface friction, as shown in the traction performance of all simulation results.

VIII. Conclusion

A new TCS strategy for obtaining maximum traction force is developed in this paper. The core contribution of this paper is the introduction of a new type of powertrain architecture for hybrid vehicles. By introducing IWMs, the front wheels can be controlled to cycle around the peak slip point. In addition, the rear wheels are controlled to track the desired wheel speed, which is defined by monitoring the cycling patterns of the front wheels, and the clutch and engine are independently controlled during this tracking step. Moreover, a special type of sliding mode control method that is free from feedback signals and that uses the nonlinear characteristics of the tires is proposed. In this way, the total number of tuning parameters is significantly reduced compared to those required in conventional TCS algorithms. Owing to the reduced number of tuning parameters and the use of simple analytical control algorithm, the computational burden of an electric control unit can be significantly reduced. Thus far, electric propulsion systems have not been able to provide a means for developing chassis control systems. However, the proposed method is expected to open up new opportunities for novel TCS algorithms. The proposed contributions here were verified through simulations.

Although the developed method has been verified only through the hybrid 4WD vehicles, pure electric vehicles or vehicles equipped with in-wheel motors are also suitable candidates for adopting the proposed strategy with little modification of algorithm.

References

[1] H. K. Roy, A. McGordon, and P. A. Jennings, "A generalized powertrain design optimization methodology to reduce fuel economy variability in hybrid electric vehicles," *IEEE Trans. Veh. Technol.*, vol. 63, no. 3, pp. 1055–1070, Mar. 2014.

[2] H. Kim and D. Kum, "Comprehensive design methodology of input- and output-split hybrid electric vehicles: In search of optimal configuration," *IEEE/ASME Trans. Mechatronics*, vol. 21, no. 6, pp. 2912–2923, Dec. 2016.

[3] X. Zhang and D. Gohlich, "A novel driving and regenerative braking regulation design based on distributed drive electric vehicles," in *Proc. 2016 IEEE Veh. Power Propulsion Conf.*, 2016, pp. 1–6.

[4] M. S. Lee, "Control method for front and rear wheel torque distribution of electric 4 wheel drive hybrid electric vehicle," U.S. Patent 20160297440A1, Oct. 13, 2016.

[5] V. Ivanov, D. Savitski, and B. Shyrokau, "A survey of traction control and antilock braking systems of full electric vehicles with individually controlled electric motors," *IEEE Trans. Veh. Technol.*, vol. 64, no. 9, pp. 3878–3896, Sep. 2015.

[6] S. Murata, "Innovation by in-wheel-motor drive unit," *Veh. Syst. Dyn.*, vol. 50, pp. 807–830, 2012.

[7] F. Borrelli, A. Bemporad, M. Fodor, and D. Hrovat, "An MPC/hybrid system approach to traction control," *IEEE Trans. Contr. Syst. Technol.*, vol. 14, no. 3, pp. 541–552, May 2006.

[8] M. Kabganian and R. Kazemi, "A new strategy for traction control in turning via engine modeling," *IEEE Trans. Veh. Technol.*, vol. 50, no. 6, pp. 1540–1548, Nov. 2001.

[9] M. Hara, S. Kamio, M. Takao, K. Sakita, and T. Abe, "Traction control system," US5018595 A, May 1991.

[10] H. Zhang, Y. Zhang, and C. Yin, "Hardware-in-the-loop simulation of robust mode transition control for a series–parallel hybrid electric vehicle," *IEEE Trans. Veh. Technol.*, vol. 65, no. 3, pp. 1059–1069, Mar. 2016.

Authorized licensed use limited to: Korea Advanced Inst of Science & Tech - KAIST. Downloaded on March 06,2020 at 11:08:26 UTC from IEEE Xplore. Restrictions apply.

[11] J. Oh, S. Choi, Y. Chang, and J. Eo, "Engine clutch torque estimation for parallel-type hybrid electric vehicles," *Int. J. Autom. Technol.*, vol. 18, pp. 125–135, 2017.

[12] R. Rajamani, G. Phanomchoeng, D. Piyabongkarn, and J. Y. Lew, "Algorithms for real-time estimation of individual wheel tire-road friction coefficients," *IEEE/ASME Trans. Mechatronics*, vol. 17, no. 6, pp. 1183–1195, Dec. 2012.

[13] C.-S. Kim, J.-O. Hahn, K.-S. Hong, and W.-S. Yoo, "Estimation of tire–road friction based on onboard 6-DoF acceleration measurement," *IEEE Trans. Veh. Technol.*, vol. 64, no. 8, pp. 3368–3377, Aug. 2015.

[14] K. S. Han, E. Lee, M. Choi, and S. B. Choi, "Adaptive scheme for the real-time estimation of tire-road friction coefficient and vehicle velocity," *IEEE/ASME Trans. Mechatronics*, vol. 22, no. 4, pp. 1508–1518, Aug. 2017.

[15] K. Han, Y. Hwang, E. Lee, and S. Choi, "Robust estimation of maximum tire-road friction coefficient considering road surface irregularity," *Int. J. Autom. Technol.*, vol. 17, pp. 415–425, 2016.

[16] J.-J. E. Slotine and W. Li, *Applied Nonlinear Control*, vol. 199. Englewood Cliffs, NJ, USA: Prentice-Hall, 1991.

[17] R. Rajamani, *Vehicle Dynamics and Control*. New York, NY, USA: Springer Science & Business Media, 2011.

[18] V. Colli, G. Tomassi, and M. Scarano, "'Single wheel' longitudinal traction control for electric vehicles," *IEEE Trans. Power Electron.*, vol. 21, no. 3, pp. 799–808, May 2006.

[19] J. J. Oh, J. S. Eo, and S. B. Choi, "Torque observer-based control of self-energizing clutch actuator for dual clutch transmission," *IEEE Trans. Contr. Syst. Technol.*, vol. 25, no. 5, pp. 1856–1864, Sep. 2017.

[20] H. K. Khalil and J. Grizzle, *Nonlinear Systems*, vol. 3. Englewood Cliffs, NJ, USA: Prentice-Hall, 1996.

[21] K. Nam, Y. Hori, and C. Lee, "Wheel slip control for improving traction-ability and energy efficiency of a personal electric vehicle," *Energies*, vol. 8, pp. 6820–6840, 2015.

[22] G. A. Magallan, C. H. De Angelo, and G. O. Garcia, "Maximization of the traction forces in a 2WD electric vehicle," *IEEE Trans. Veh. Technol.*, vol. 60, no. 2, pp. 369–380, Feb. 2011.

[23] B. Subudhi and S. S. Ge, "Sliding-mode-observer-based adaptive slip ratio control for electric and hybrid vehicles," *IEEE Trans. Intell. Transp. Syst.*, vol. 13, no. 4, pp. 1617–1626, Dec. 2012.

[24] R. Kunii, A. Iwazaki, Y. Atsumi, and A. Mori, "Development of SH-AWD (super handling-all wheel drive) system," *Honda R D Tech. Rev.*, vol. 16, pp. 9–16, 2004.

[25] P. A. Ioannou and J. Sun, *Robust Adaptive Control*. North Chelmsford, MA, USA: Courier Corporation, 2012.

[26] H. Pacejka, *Tire and Vehicle Dynamics*. Amsterdam, The Netherlands: Elsevier, 2005.

Kyoungseok Han received the bachelor's degree in civil engineering (minor in mechanical engineering) from Hanyang University, Seoul, South Korea, in 2013, and the master's degree in mechanical engineering from Korea Advanced Institute of Science and Technology, Daejeon, South Korea, where he is currently working toward the Ph.D. degree in mechanical engineering. His current research interests include vehicle dynamics and control, vehicle state estimation, and control theory.

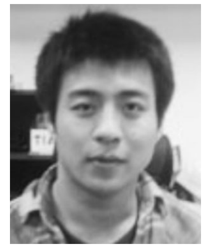

Mooryong Choi received the B.S. degree in mechanical engineering from Yonsei University, Seoul, South Korea, in 2008, the M.S. degree in mechanical engineering from the University of California, Los Angeles, CA, USA, in 2010, and the Ph.D degree in mechanical engineering from Korea Advanced Institute of Science and Technology, Daejeon, South Korea, in 2014. He is currently with Hyundai-Kia R&D Center, Seoul. His research interests include vehicle dynamics, control, and computer vision.

Byunghwan Lee received the B.S. and M.S. degrees in electronic, electrical, and computer engineering from Hanyang University, Seoul, South Korea, in 2011 and 2013, respectively. He is currently with Hyundai-Kia R&D Center, Seoul. His research interests include vehicle dynamics and hybrid electric vehicle control.

Seibum B. Choi (M'09) received the B.S. degree in mechanical engineering from Seoul National University, Seoul, South Korea, in 1985, the M.S. degree in mechanical engineering from Korea Advanced Institute of Science and Technology (KAIST), Daejeon, South Korea, in 1987, and the Ph.D. degree in control from the University of California, Berkeley, CA, USA, in 1993. From 1993 to 1997, he was involved in the development of automated vehicle control systems with the Institute of Transportation Studies, University of California. During 2006, he was with TRW, Warren, MI, USA, where he was involved in the development of advanced vehicle control systems. Since 2006, he has been with the Faculty of the Mechanical Engineering Department, KAIST. His current research interests include fuel-saving technology, vehicle dynamics and control, and active safety systems.

Authorized licensed use limited to: Korea Advanced Inst of Science & Tech - KAIST. Downloaded on March 06,2020 at 11:08:26 UTC from IEEE Xplore. Restrictions apply.